GEOLOGY | THE GEOLOGICAL SOCIETY OF AMERICA®

https://doi.org/10.1130/G48503.1

Manuscript received 12 October 2020
Revised manuscript received 25 February 2021
Manuscript accepted 2 March 2021

Published online 28 April 2021

History of the Larsen C Ice Shelf reconstructed from sub–ice shelf and offshore sediments

J.A. Smith[1], C.-D. Hillenbrand[1], C. Subt[2], B.E. Rosenheim[3], T. Frederichs[4,5], W. Ehrmann[6], T.J. Andersen[7], L. Wacker[8], K. Makinson[1], P. Anker[1], E.J. Venables[9] and K.W. Nicholls[1]

[1]British Antarctic Survey, High Cross, Madingley Road, Cambridge CB3 0ET, UK
[2]Department of Geology, El Paso Community College, El Paso, Texas 79915, USA
[3]College of Marine Science, University of South Florida, St. Petersburg, Florida 33701, USA
[4]Faculty of Geosciences, University of Bremen, Bremen 28359, Germany
[5]MARUM–Center for Marine Environmental Sciences, University of Bremen, 28359 Bremen, Germany
[6]Institute for Geophysics & Geology, University of Leipzig, Leipzig 04103, Germany
[7]Department of Geosciences & Natural Resource Management, University of Copenhagen, 1350 Copenhagen, Denmark
[8]ETH Zürich, Laboratory of Ion Beam Physics, 8093 Zurich, Switzerland
[9]Department of Arctic and Marine Biology, UiT Arctic University of Norway, N-9037 Tromsø, Norway

ABSTRACT

Because ice shelves respond to climatic forcing over a range of time scales, from years to millennia, an understanding of their long-term history is critically needed for predicting their future evolution. We present the first detailed reconstruction of the Larsen C Ice Shelf (LCIS), eastern Antarctic Peninsula (AP), based on data from sediment cores recovered from below and in front of the ice shelf. Sedimentologic and chronologic information reveals that the grounding line (GL) of an expanded AP ice sheet had started its retreat from the midshelf prior to 17.7 ± 0.53 calibrated (cal.) kyr B.P., with the calving line following ~6 k.y. later. The GL had reached the inner shelf as early as 9.83 ± 0.85 cal. kyr B.P. Since ca. 7.3 ka, the ice shelf has undergone two phases of retreat but without collapse, indicating that the climatic limit of LCIS stability was not breached during the Holocene. Future collapse of the LCIS would therefore confirm that the magnitudes of both ice loss along the eastern AP and underlying climatic forcing are unprecedented during the past 11.5 k.y.

INTRODUCTION

The Larsen C Ice Shelf (LCIS) is the largest remaining ice shelf on the Antarctic Peninsula (AP) and is thought to be the next in line to collapse under continued climatic warming (Jansen et al., 2015). The sequential breakup of ice shelves along the eastern AP (Fig. 1A) has been linked to the southward migration of the −9 °C mean annual isotherm, considered to be the "climatic limit" of ice-shelf stability (Morris and Vaughan, 2003). Above this limit, surface melting is enhanced, and ice shelves are more vulnerable to collapse through a range of processes, e.g., hydrofracture, as demonstrated by the rapid disintegration of the Larsen B Ice Shelf (LBIS) in 2002 (Scambos et al., 2003). Satellite data also indicate that the LBIS thinned in the decades leading up to its collapse, likely as a result of enhanced ocean-driven melting (Shepherd et al., 2003). The –9°C isotherm sits at the northern end of the LCIS (Fig. 1) and it has been suggested that as thinning progresses, the ice shelf could reach a critical tipping point, leading to rapid disintegration (Holland et al., 2015). Tipping points include unpinning from Bawden Ice Rise (Fig. 1) (Borstad et al., 2013; Adusumilli et al., 2018), retreat of the ice shelf front to an unstable configuration (Kulessa et al., 2014), and/or hydrofracture driven by increased surface melting associated with Föhn (warm, dry, downslope) winds (Luckman et al., 2014). Together with an improved understanding of the drivers of contemporary retreat, the collapse of AP ice shelves also enabled the recovery and analysis of previously inaccessible marine records. Research revealed that the Prince Gustav Channel (PGC) (Pudsey and Evans, 2001) and Larsen A (LAIS) (Brachfeld et al., 2003) ice shelves collapsed during the mid–late Holocene (ca. 6.0–2.0 cal. kyr B.P.), whereas the LBIS remained stable (Domack et al., 2005). Persistence of the LBIS provided the first suggestions that contemporary ice-shelf loss, certainly along the eastern AP, was unprecedented during the past 11.5 k.y. (Domack et al., 2005). Furthermore, the oxygen isotope composition of planktic foraminifera in a core from the Larsen B embayment also provided evidence that the LBIS thinned prior to its collapse (Domack et al., 2005). Although the history of this thinning is poorly constrained by chronological data, Mulvaney et al. (2012) suggested that the rise in atmospheric temperatures since ca. 0.5 ka, observed in the James Ross Island Ice core (Fig. 1), likely rendered eastern AP ice shelves more vulnerable to collapse. In other words, some ice shelves might be preconditioned to collapse by decades (Shepherd et al., 2003), centuries (Mulvaney et al., 2012), or even millennia of thinning (Domack et al., 2005).

Little is known about the pre-satellite history of the LCIS, leaving a significant gap in our understanding of past ice-shelf retreats. Either it has collapsed in the past, challenging the idea that contemporary retreat is unprecedented during the Holocene, or it has remained stable. Stability would solidify the idea that contemporary ice loss, and the climate variability driving it, now exceeds the natural changes of the Holocene. We addressed this knowledge gap by analyzing sediment core LN2 recovered from beneath the LCIS and combined this data set with new chronological information from legacy marine core VC331, collected ~15 km in front of the ice shelf (Fig. 1B) (Curry and Pudsey, 2007).

CITATION: Smith, J.A., et al., 2021, History of the Larsen C Ice Shelf reconstructed from sub–ice shelf and offshore sediments: Geology, v. 49, p. 978–982, https://doi.org/10.1130/G48503.1

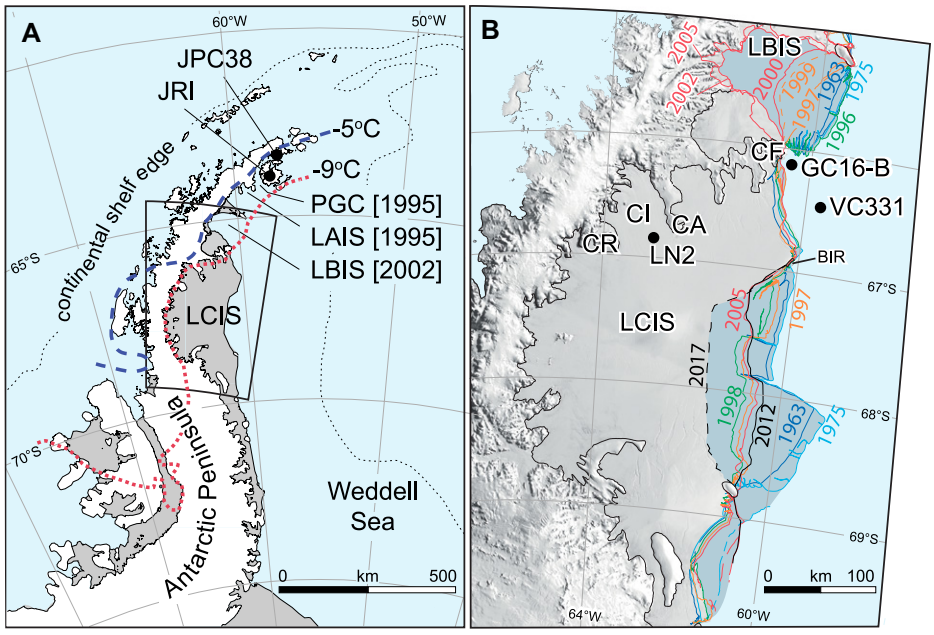

Figure 1. (A) Map of the Antarctic Peninsula (AP) showing Prince Gustav Channel (PGC), Larsen A (LAIS), Larsen B (LBIS), and Larsen C (LCIS) ice shelves, James Ross Island (JRI) ice core, and sediment core JPC38. Year of contemporary collapse is given in brackets. Red dotted and blue dashed line refer to –9 °C and –5 °C isotherms, respectively (Morris and Vaughan, 2003). (B) Map of LCIS showing cores LN2, VC331, and GC16-B, and Cabinet Inlet (CI), Cape Roberts (CR), Cape Alexander (CA), Cape Framnes (CF), and Bawden ice rise (BIR). Colored lines show historical calving line positions.

MATERIALS

An access hole was drilled through the LCIS in 2012 using the British Antarctic Survey (BAS) hot-water drill system. Core LN2 (66°52.0′S, 62°54.0′W) was recovered using a UWITEC percussion corer from a broad bathymetric trough (Brisbourne et al., 2020). Analyses of core LN2 included grain size, magnetic susceptibility (MS), total organic carbon (TOC), X-radiographs, X-ray fluorescence (XRF) scanning, and clay mineralogy (see the Supplemental Material[1]). To obtain a chronology for LN2, we applied conventional accelerator mass spectrometry (AMS) radiocarbon (^{14}C) dating of calcareous microfossils and the acid insoluble organic (AIO) fraction, ramped pyrolysis (PyrOx) ^{14}C dating (Rosenheim et al., 2008; Subt et al., 2017), relative paleointensity (RPI), and ^{210}Pb dating. Radiocarbon ages are quoted as calibrated (cal.) kyr B.P., whereas RPI ages are quoted as kiloannum (ka).

Vibrocore VC331 (66°26.1′S, 59°57.6′W) was recovered during expedition JR71 in 2002 (Fig. 1B) and described by Curry and Pudsey (2007). It consists of a deformation till at its base (465–420 cm) associated with grounded ice, a sub–ice shelf proximal (420–375 cm) to distal grounding line (GL) facies (375–50 cm), and a bioturbated open-marine facies (50–0 cm), with elevated concentrations of ice-rafted debris and foraminifera near the top (Fig. 2B) (Curry and Pudsey, 2007). We applied ramped PyrOx ^{14}C dating to this hitherto undated core.

RESULTS AND DISCUSSION

Lithology and Paleoenvironmental Interpretation of Core LN2

Core LN2 consists of five lithological units (Figs. 2A and 2C). The basal unit V is a weakly stratified, muddy diamicton with common gravel- to pebble-sized clasts, low TOC, and low bromine contents (Br; used here as a proxy for marine organic matter; e.g., Smith et al., 2017). Unit V is overlain by the ~10-cm-thick unit IV, which consists of laminated mud characterized by an absence of sand and gravel, a MS minimum, and maxima in Br, TOC, and kaolinite. Unit III is a laminated to massive sandy mud. It shares similar characteristics to unit V but is finer grained. TOC, Br, and kaolinite decrease relative to unit IV. Unit II is a laminated mud with dispersed gravel. Like in unit IV, TOC, Br, and kaolinite reach maxima that correlate with MS minima. Unit I consists of laminated to massive sandy mud with dispersed gravel. TOC and Br are lower than in the underlying unit but increase toward the core top. Unit I is moderately bioturbated in the upper ~15 cm, where the sediments contain low numbers of calcareous planktic and benthic foraminifera, ostracods and fragments of gastropods, bryozoans, and serpulid worm tubes. A notable feature of units II and I is an up-core increase in MS and chlorite (Fig. 2).

The coarse-grained nature, weak stratification, and low shear strength of unit V indicate deposition in a GL proximal environment (Domack and Harris, 1998; Powell et al., 1996). The lack of microfossils and low TOC content are typical of ice-shelf cover (Smith et al., 2019). The transition from diamicton to finer-grained, laminated mud (units V to IV) implies retreat of the GL (Powell et al., 1996). Concurrent increases in TOC and Br imply that retreat of the GL was accompanied by retreat of the calving line, increasing the supply of marine particles to site LN2 (e.g., Smith et al., 2019). Coarsening in unit III, relative to unit IV, is interpreted to reflect a modest GL readvance, with the GL further away from the core site than during deposition of unit V. Low values of TOC and Br indicate reduced influence from the open ocean, likely as a result of ice-shelf expansion. Unit II is similar in nature to unit IV, and it suggests a further episode of GL and calving line retreat, reflected in finer grain size and elevated organic content, respectively. The higher sand content and clast abundance in unit I can be explained by (1) increased winnowing, (2) increased melt-out of debris from the ice-shelf base, or (3) readvance of the GL toward the core site. Significant winnowing is at odds with the ^{210}Pb data (below), which corroborate the presence of modern seafloor surface sediments. Furthermore, unlike units V and III, which represent GL proximal sedimentation, the grain-size composition of unit I is dominated by 2–8-mm-sized clasts in a muddy matrix, which is typical of rain-out of debris from an overhanging ice shelf (Domack and Harris, 1998). Thus, we attribute the coarsening of unit I to increased sub–ice shelf melting, although a minor GL advance or increased winnowing cannot be ruled out. Finally, the decrease of TOC in the lower part of unit I and increase toward its top (Fig. 2) indicate variable inputs of marine particles, which we attribute to an ice-shelf front advance and then retreat to the modern position. Changes in clay mineralogy, which provide information on sediment provenance, also help to constrain the GL position during deposition of units II and I. The AP acts as a source for illite and chlorite (Hillenbrand et al., 2003), and analysis of surface sediments indicates that chlorite is much higher in this region than sediment sourced from further to the south and east within the Weddell Gyre (Petschick et al., 1996). Thus, the gradual increase in chlorite from ~45 cm could reflect retreat of the GL toward its modern position, with glacier erosion focused on the AP. Concurrent increases in MS are consistent with this interpretation, since detritus delivered from the coast in Cabinet Inlet is predominantly sourced from highly magnetic bedrock (Wendt et al., 2013).

[1]Supplemental Material. Figures S1–S4 (RPI data), Figures S5–S6 (^{14}C and ^{210}Pb data), Table S1 (rock magnetic parameters), Tables S2–S3 (radiocarbon dates), chronology, sedimentological methods, and supplemental references. Please visit https://doi.org/10.1130/GEOL.S.14390690 to access the supplemental material, and contact editing@geosociety.org with any questions.

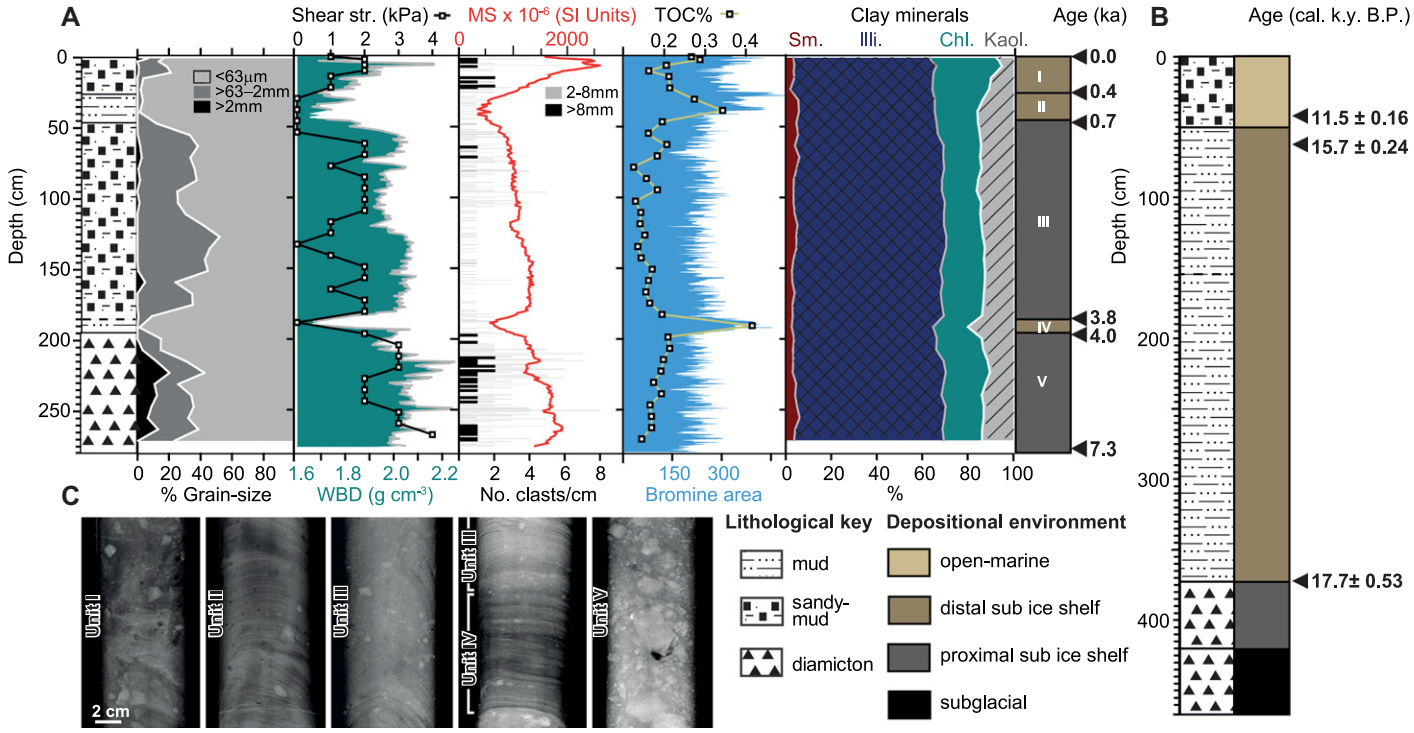

Figure 2. (A) Core data for LN2 (Larsen C Ice Shelf, 66°52.0′S, 62°54.0′W). Relative paleointensity (RPI) ages (ka) are given alongside five lithological units/depositional environments. WBD—wet-bulk density, MS—magnetic susceptibility, TOC—total organic carbon, Sm—smectite, Illi—illite, Chl—chlorite, Kaol—kaolinite. (B) Core lithology (adapted from Curry and Pudsey, 2007) and ramped pyrolysis (PyrOx) ^{14}C ages (cal. kyr B.P.) for core VC331 (66°26.1′S, 59°57.6′W). (C) X-radiographs of lithological units (I–V) in core LN2.

Chronology

Core LN2

The ^{210}Pb dating indicates that core LN2 recovered modern seafloor surface sediments (Fig. S5B). Down-core AIO ^{14}C dates yielded anomalously old ages, likely due to the incorporation of fossil carbon (Fig. S5A; Table S2). Attempts to mitigate these effects using ramped PyrOx ^{14}C dating were unsuccessful (Table S2; Supplemental Material). Because of these issues, the LN2 chronology is based on RPI data tuned to an RPI curve from the northwestern AP shelf, which was itself dated through correlation with ^{14}C-constrained RPI records (Willmott et al., 2006). Accuracy of the age model for core LN2 is therefore limited to that of the tuning target (see the Supplemental Material). Our age model yielded the following ages for core LN2, with an uncertainty of ±0.25 ka: unit V = 7.3–4.0 ka; unit IV = 4.0–3.8 ka; unit III = 3.8–0.7 ka; unit II = ca. 0.7–0.4 ka, and unit I = 0.4 ka to present. The uncertainty is derived from the average uncertainty in the Willmott et al. (2006) data set.

In addition, calcareous microfossils (bryozoan, gastropod fragments, benthic and planktic foraminifera) in the upper 12 cm of LN2 yielded calibrated ^{14}C ages of 7.9 ± 0.14–9.8 ± 0.85 cal. kyr B.P. (Table S2). Such ages are enigmatic and are inconsistent with the ^{210}Pb data, which indicate the presence of modern seafloor surface sediments. We argue that the inner shelf was colonized by a diverse benthic assemblage soon after the GL retreated at 9.8 ± 0.85 cal. kyr B.P. At the same time, low numbers of planktic foraminifera were advected beneath the ice shelf from the open ocean. Later, the material was remobilized by the ice shelf, probably by freeze-on (Nicholls et al., 2012), and transported to site LN2, where it subsequently melted out from the ice-shelf base.

Core VC331

Down-core AIO ^{14}C dates in VC331 are also anomalously old (Fig. S6; Table S2). Ramped PyrOx ^{14}C dating indicates that the subglacial to glacimarine transition occurred after 17.7 ± 0.53 cal. kyr B.P. (Fig. 2). Open-marine sedimentation was established by 11.5 ± 0.16 cal. kyr B.P., although it is likely that the calving line was close to the core site by 15.7 ± 0.24 cal. kyr B.P. and remained nearby for ~4.0 k.y. (Fig. 2). This is suggested by enhanced coarse detritus from ~130 to 30 cm (Curry and Pudsey, 2007, their figure 4), which is typical of calving line deposition (Smith et al., 2019).

Evolution of the LCIS since the Last Glacial Maximum

Chronological data from cores LN2 and VC331 were then combined with published ramped PyrOx ^{14}C dates from nearby core GC16-B (Fig. 1B; Fig. S7; Subt et al., 2017) to reconstruct the evolution of the LCIS since the Last Glacial Maximum. Results indicate that the AP ice sheet retreated from site VC331 just before or at ca. 17.7 ± 0.53 cal. kyr B.P., with the calving line of a fringing ice shelf situated close to the site after ca. 15.7 ± 0.24 cal. kyr B.P. (Figs. 3). The GL had retreated landward of GC16-B by 11.5 ± 0.47 cal. kyr B.P., with ice-shelf cover persisting until ca. 4.1 ± 0.07 cal. kyr B.P. After ca. 11.5 ± 0.16 cal. kyr B.P., open-marine conditions were established at site VC331. Before ca. 9.8 ± 0.85 cal. kyr B.P., the GL retreated to a position landward of LN2, with the calving line situated to the east of site GC16-B. There is limited published information on ice-sheet thickness changes in the Larsen C sector, although exposure age dating of rocks on the northern slope of Cape Framnes (Fig. 1B) suggests that GL retreat during this period was also likely accompanied by ice-sheet thinning until ca. 6.0 ka (Jeong et al., 2018). Deposition of coarse-grained sediments at site LN2 between ca. 7.3 and ca. 4.0 ka indicates a stationary GL, probably located close to the core site (e.g., Powell et al., 1996). This was followed by GL and calving line retreat between ca. 4.0 and ca. 3.8 ka, with the calving line retreating landward of site GC16-B. Furthermore, because concentrations of Br and TOC in core LN2 are higher in sediments deposited during this interval relative to modern surface sediments, it is likely that the calving line retreated upstream from its 2012 position, i.e., when the core was recovered. This would have increased the delivery of marine

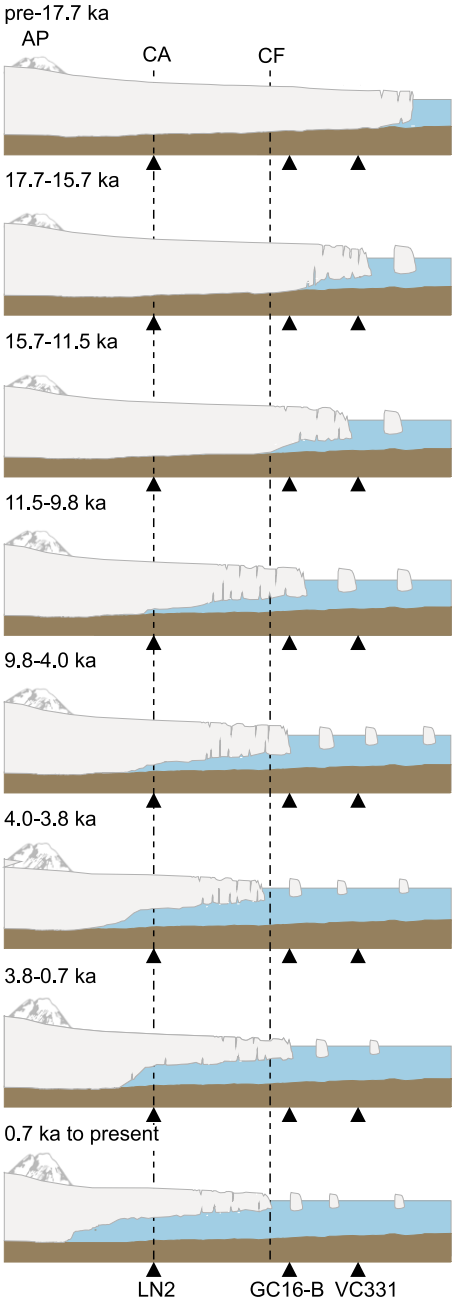

Figure 3. Reconstruction of the Larsen C Ice Shelf (LCIS) ca. 17.7 ka to present. Vertical lines denote relative positions of Cape Alexander (CA) and Cape Framnes (CF). Antarctic Peninsula (AP) is also shown. Ages for core GC16-B are from Subt et al. (2017), and ice-sheet thinning is inferred from Jeong et al. (2018).

particles to site LN2 (McKay et al., 2016). The GL remained largely stationary between ca. 3.8 and ca. 0.7 ka. At some time after ca. 0.7 ka, the GL retreated to a position similar to present, with the ice shelf potentially undergoing a phase of increased thinning. Unfortunately, the timing of these changes is uncertain due to the limitations of our age model. We note that ice-shelf thinning after ca. 0.7 ka is broadly consistent with $\delta^{18}O_{diatom}$ data from the South Orkney shelf, interpreted to reflect enhanced melting of eastern AP ice shelves during the past ~0.3 k.y. (Dickens et al., 2019). Finally, increases of TOC in core LN2 at ca. 0.7 ka and of both Br and TOC after ca. 0.5 ka indicate closer proximity of an open-ocean source for marine particles, which we attribute to retreat-advance-retreat of the calving line (see Fig. 1B). This phase of calving line retreat starting at ca. 0.7 ka progressed upstream of the 2012 ice-shelf front. How far upstream remains to be determined, as this would involve sampling sediment proximal or adjacent to the current LCIS front following the calving of iceberg A-68 in 2017.

Persistence of the LCIS throughout the Holocene

Analyses of sub–ice shelf core LN2 revealed that the GL of an expanded AP ice sheet had retreated to the inner Larsen C shelf by ca. 9.8 cal. kyr B.P. Notably, the LCIS did not collapse during the Holocene, although its front did undergo two episodes of retreat at ca. 4.0–3.8 ka and after ca. 0.7 ka. Frontal retreat without collapse supports the hypothesis that the LCIS has a large "passive" frontal zone that, if lost, has little dynamic influence on the ice shelf (Fürst et al., 2016). Similar to contemporary ice-shelf loss, there is a north-south trend in the timing of past breakup and retreat events (Fig. 4). However, whereas contemporary ice-shelf collapses have been near-synchronous (Hodgson, 2011), the southward progression of Holocene retreats was gradual, spanning thousands of years. The timing of GL retreat to the inner shelf also shows a north-south trend, although there is uncertainty with these ages. The persistence of the LCIS and LBIS throughout the Holocene indicates that these ice shelves were (1) more resilient to climate forcing, possibly because they were thicker (Domack et al., 2005), (2) buffered by remnant ice domes on the continental shelf (Jeong et al., 2018), or (3) the magnitude of forcing south of ~65°S was insufficient to destabilize them, or a combination of all three factors. In this context, Holocene collapses of the LAIS and PGC have been attributed to atmospheric warming between ca. 6 and 2.5 ka, when air temperatures were similar to, or exceeded, modern-day values (Fig. 4). In contrast, there is no clear association between the recent TEX_{86}^{L}-based (tetraether index of 86 carbon atoms, where L is low temperature) surface-ocean temperature reconstruction (JPC38; Fig. 1A) and the timing of Holocene ice-shelf retreat (Fig. 4), although warming between ca. 8.2 and 7.0 cal. kyr B.P. might have left the LAIS and PGC more vulnerable to collapse (Fig. 4; Etourneau et al., 2019). However, not all proxy records are consistent with this TEX_{86}^{L}-based reconstruction, with diatom data indicating enhanced productivity and potentially warmer ocean conditions ca. 7.2–2.5 cal. kyr B.P. (Minzoni et al., 2015). Thus, there is an urgent need for additional proxy work to help tease apart the relative contributions of atmospheric and oceanic melting in driving past retreats on the eastern AP. A key difference between Holocene and contemporary ice-shelf retreat could be the magnitude of ocean-induced melting, which contributed to recent collapse of the LAIS and LBIS (Shepherd et al., 2003) and is currently contributing to the thinning of the LCIS (Adusumilli et al., 2018; Holland et al., 2015).

ACKNOWLEDGMENTS

This research has been supported by the British Antarctic Survey's, Polar Science for Planet Earth programme and NERC grant NE/H009205/1. We are indebted to Mike Brian for his support in the field. Finally, we thank Stefanie Brachfeld, Rob McKay, and Becky Minzoni for their constructive reviews that improved our paper.

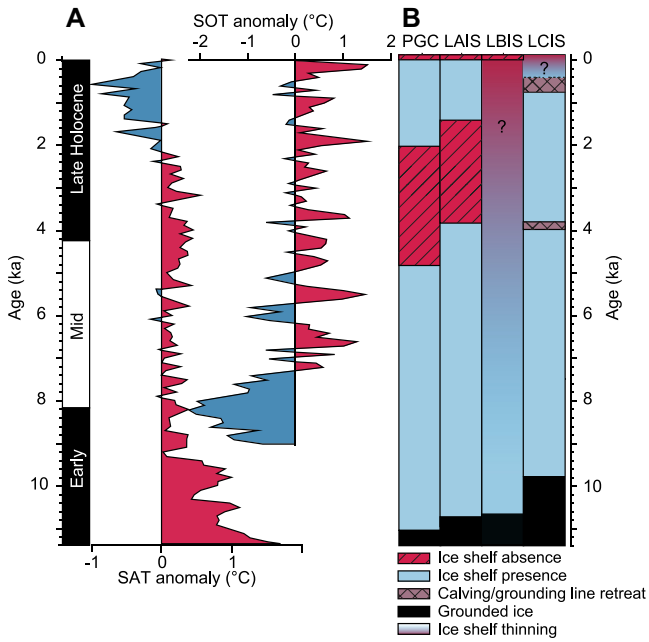

Figure 4. (A) Reconstructed surface air temperature (SAT) (Mulvaney et al., 2012) and surface ocean temperature (SOT) (Etourneau et al., 2019), plotted as positive/negative anomalies from 0 °C. (B) Holocene history of Prince Gustav Channel (PGC) (Pudsey and Evans, 2001), Larsen A Ice Shelf (LAIS) (Brachfeld et al., 2003), Larsen B Ice Shelf (LBIS) (Domack et al., 2005; Jeong et al., 2018), and Larsen C Ice Shelf (LCIS) (this study). Onset of thinning of LBIS (Domack et al., 2005) and late Holocene thinning and retreat of LCIS are uncertain.

REFERENCES CITED

Adusumilli, S., Fricker, H.A., Siegfried, M.R., Padman, L., Paolo, F.S., and Ligtenberg, S.R.M., 2018, Variable basal melt rates of Antarctic Peninsula ice shelves, 1994–2016: Geophysical Research Letters, v. 45, p. 4086–4095, https://doi.org/10.1002/2017GL076652.

Borstad, C P., Rignot, E., Mouginot, J., and Schodlok, M.P., 2013, Creep deformation and buttressing capacity of damaged ice shelves: theory and application to Larsen C ice shelf: Cryosphere, v. 7, p. 1931–1947, https://doi.org/10.5194/tc-7-1931-2013.

Brachfeld, S., Domack, E., Kissel, C., Laj, C., Leventer, A., Ishman, S., Gilbert, R., Camerlenghi, A., and Eglinton, L.B., 2003, Holocene history of the Larsen-A ice shelf constrained by geomagnetic paleointensity dating: Geology, v. 31, p. 749–752, https://doi.org/10.1130/G19643.1.

Brisbourne, A., Kulessa, B., Hudson, T., Harrison, L., Holland, P., Luckman, A., Bevan, S., Ashmore, D., Hubbard, B., Pearce, E., White, J., Booth, A., Nicholls, K., and Smith, A., 2020, An updated seabed bathymetry beneath Larsen C ice shelf, Antarctic Peninsula: Earth System Science Data, v. 12, p. 887–896, https://doi.org/10.5194/essd-12-887-2020.

Curry, P., and Pudsey, C.J., 2007, New Quaternary sedimentary records from near the Larsen C and former Larsen B ice shelves: Evidence for Holocene stability: Antarctic Science, v. 19, no. 3, p. 355–364, https://doi.org/10.1017/S0954102007000442.

Dickens, W.A., Kuhn, G., Leng, M.J., Graham, A.G.C., Dowdeswell, J.A., Meredith, M.P., Hillenbrand, C.D., Hodgson, D.A., Roberts, S.J., Sloane, H., and Smith, J.A., 2019, Enhanced glacial discharge from the eastern Antarctic Peninsula since the 1700s associated with a positive Southern Annular Mode: Scientific Reports, v. 9, p. 14606, https://doi.org/10.1038/s41598-019-50897-4.

Domack, E., and Harris, P.T., 1998, A new depositional model for ice shelves, based upon sediment cores from the Ross Sea and the MaC. Robertson shelf, Antarctica: Annals of Glaciology, v. 27, p. 281–284.

Domack, E., Duran, D., Leventer, A., Ishman, S., Doane, S., McCallum, S., Amblas, D., Ring, J., Gilbert, R., and Prentice, M., 2005, Stability of the Larsen B ice shelf on the Antarctic Peninsula during the Holocene Epoch: Nature, v. 436, p. 681–685, https://doi.org/10.1038/nature03908.

Etourneau, J., et al., 2019, Ocean temperature impact on ice shelf extent in the eastern Antarctic Peninsula: Nature Communications, v. 10, p. 304, https://doi.org/10.1038/s41467-018-08195-6.

Fürst, J.J., Durand, G., Gillet-Chaulet, F., Tavard, L., Rankl, M., Braun, M., and Gagliardini, O., 2016, The safety band of Antarctic ice shelves: Nature Climate Change, v. 6, p. 479–482, https://doi.org/10.1038/nclimate2912.

Hillenbrand, C.D., Grobe, H., Diekmann, B., Kuhn, G., and Futterer, D.K., 2003, Distribution of clay minerals and proxies for productivity in surface sediments of the Bellingshausen and Amundsen Seas (West Antarctica)—Relation to modern environmental conditions: Marine Geology, v. 193, p. 253–271, https://doi.org/10.1016/S0025-3227(02)00659-X.

Hodgson, D.A., 2011, First synchronous retreat of ice shelves marks a new phase of polar deglaciation: Proceedings of the National Academy of Sciences of the United States of America, v. 108, p. 18859–18860, https://doi.org/10.1073/pnas.1116515108.

Holland, P.R., Brisbourne, A., Corr, H.F.J., McGrath, D., Purdon, K., Paden, J., Fricker, H.A., Paolo, F.S., and Fleming, A.H., 2015, Oceanic and atmospheric forcing of Larsen C ice-shelf thinning: The Cryosphere, v. 9, no. 3, p. 1005–1024, https://doi.org/10.5194/tc-9-1005-2015.

Jansen, D., Luckman, A.J., Cook, A., Bevan, S., Kulessa, B., Hubbard, B., and Holland, P.R., 2015, Brief Communication: Newly developing rift in Larsen C ice shelf presents significant risk to stability: The Cryosphere, v. 9, no. 3, p. 1223–1227, https://doi.org/10.5194/tc-9-1223-2015.

Jeong, A., Il Lee, J., Seong, Y.B., Balco, G., Yoo, K.C., Il Yoon, H., Domack, E., Rhee, H.H., and Yu, B.Y., 2018, Late Quaternary deglacial history across the Larsen B embayment, Antarctica: Quaternary Science Reviews, v. 189, p. 134–148, https://doi.org/10.1016/j.quascirev.2018.04.011.

Kulessa, B., Jansen, D., Luckman, A.J., King, E.C., and Sammonds, P.R., 2014, Marine ice regulates the future stability of a large Antarctic ice shelf: Nature Communications, v. 5, 3707, https://doi.org/10.1038/ncomms4707.

Luckman, A., Elvidge, A., Jansen, D., Kulessa, B., Kuipers Munneke, P., King, J., and Barrand, N., 2014, Surface melt and ponding on Larsen C Ice Shelf and the impact of föhn winds: Antarctic Science, v. 26, p. 625–635, https://doi.org/10.1017/S0954102014000339.

McKay, R., Golledge, N.R., Maas, S., Naish, T., Levy, R., Dunbar, G., and Kuhn, G., 2016, Antarctic marine ice-sheet retreat in the Ross Sea during the early Holocene: Geology, v. 44, p. 7–10, https://doi.org/10.1130/G37315.1.

Minzoni, R.T., Anderson, J.B., Fernandez, R., and Wellner, J.S., 2015, Marine record of Holocene climate, ocean, and cryosphere interactions: Herbert Sound, James Ross Island, Antarctica: Quaternary Science Reviews, v. 129, p. 239–259, https://doi.org/10.1016/j.quascirev.2015.09.009.

Morris, E.M., and Vaughan, D.G., 2003, Spatial and temporal variation of surface temperature on the Antarctic Peninsula and the limit of variability of ice shelves, *in* Domack, E., et al., eds., Antarctic Peninsula Climate Variability: Historical and Paleoenvironmental Perspectives: American Geophysical Union Antarctic Research Series 79, p. 61–69.

Mulvaney, R., Abram, N.J., Hindmarsh, R.C.A., Arrowsmith, C., Fleet, L., Triest, J., Sime, L.C., Alemany, O., and Foord, S., 2012, Recent Antarctic Peninsula warming relative to Holocene climate and ice-shelf history: Nature, v. 489, p. 141–144, https://doi.org/10.1038/nature11391.

Nicholls, K.W., Corr, H.F.J., Makinson, K., and Pudsey, C.J., 2012, Rock debris in an Antarctic ice shelf: Annals of Glaciology, v. 53, p. 235–240, https://doi.org/10.3189/2012AoG60A014.

Petschick, R., Kuhn, G., and Gingele, F., 1996, Clay mineral distribution in surface sediments of the South Atlantic: Sources, transport, and relation to oceanography: Marine Geology, v. 130, p. 203–229, https://doi.org/10.1016/0025-3227(95)00148-4.

Powell, R.D., Dawber, M., McInnes, J.N., and Pyne, A.R., 1996, Observations of the grounding-line area at a floating glacier terminus: Annals of Glaciology, v. 22, p. 217–223.

Pudsey, C.J., and Evans, J., 2001, First survey of Antarctic sub–ice shelf sediments reveals mid-Holocene ice shelf retreat: Geology, v. 29, p. 787–790, https://doi.org/10.1130/0091-7613(2001)029<0787:FSOASI>2.0.CO;2.

Rosenheim, B.E., Day, M.B., Domack, E., Schrum, H., Benthien, A., and Hayes, J.M., 2008, Antarctic sediment chronology by programmed-temperature pyrolysis: Methodology and data treatment: Geochemistry Geophysics Geosystems, v. 9, Q04005, https://doi.org/10.1029/2007GC001816.

Scambos, T., Hulbe, C., and Fahnestock, M., 2003, Climate-induced ice shelf disintegration in the Antarctic Peninsula, *in* Domack, E., et al., eds., Antarctic Peninsula Climate Variability: Historical and Paleoenvironmental Perspectives: American Geophysical Union Antarctic Research Series 79, p. 79–92, https://doi.org/10.1029/AR079p0079.

Shepherd, A., Wingham, D., Payne, T., and Skvarca, P., 2003, Larsen ice shelf has progressively thinned: Science, v. 302, p. 856–859, https://doi.org/10.1126/science.1089768.

Smith, J.A., Andersen, T.J.A., Shortt, M., Gaffney, A.M., Truffer, M., Stanton, T.P., Bindschadler, R., Dutrieux, P., Enkins, A.J., Hillenbrand, C.D., Ehrmann, W., Corr, H.F.J., Farley, N., Crowhurst, S., and Vaughan, D.G., 2017, Sub-ice-shelf sediments record history of twentieth-century retreat of Pine Island Glacier: Nature, v. 541, p. 77–80, https://doi.org/10.1038/nature20136.

Smith, J.A., Graham, A.G.C., Post, A.L., Hillenbrand, C.D., Bart, P.J., and Powell, R.D., 2019, The marine geological imprint of Antarctic ice shelves: Nature Communications, v. 10, p. 5635, https://doi.org/10.1038/s41467-019-13496-5.

Subt, C., Yoon, H.I., Yoo, K.C., Lee, J.I., Leventer, A., Domack, E.W., and Rosenheim, B.E., 2017, Sub–ice shelf sediment geochronology utilizing novel radiocarbon methodology for highly detrital sediments: Geochemistry Geophysics Geosystems, v. 18, p. 1404–1418, https://doi.org/10.1002/2016GC006578.

Wendt, A.S., Vaughan, A.P.M., Ferraccioli, F., and Grunow, A.M., 2013, Magnetic susceptibilities of rocks of the Antarctic Peninsula: Implications for the redox state of the batholith and the extent of metamorphic zones: Tectonophysics, v. 585, p. 48–67, https://doi.org/10.1016/j.tecto.2012.07.011.

Willmott, V., Domack, E.W., Canals, M., and Brachfeld, S., 2006, A high resolution relative paleointensity record from the Gerlache-Boyd paleo–ice stream region, northern Antarctic Peninsula: Quaternary Research, v. 66, p. 1–11, https://doi.org/10.1016/j.yqres.2006.01.006.

Printed in USA